Plant Nano Biology 8 (2024) 100072

Contents lists available at ScienceDirect

Plant Nano Biology

journal homepage: www.journals.elsevier.com/plant-nano-biology

Tb-doped strontium aluminate nanophosphor: Cytotoxicity, phytotoxicity, and bioimaging in plant cells

Neenu Mary Thomas [a,b,c], Naijil George [d], M.O. Viji [d], E.I Anila [c,e,*]

[a] Department of Physics, Morning Star Home Science College, Angamaly, Ernakulam, Kerala 683573, India
[b] Center for Nano-Bio Polymer Science and Technology, Department of Physics, St. Thomas College, Palai, Arunapuram, Kottayam, Kerala 686574, India
[c] Optoelectronic and Nanomaterials' Research Lab, Department of Physics, Union Christian College, Aluva, Ernakulam, Kerala 683102, India
[d] Department of Biotechnology, St. Joseph's College (Autonomous), Irinjalakuda (Affiliated to the University of Calicut), Kerala 680121, India
[e] Department of Physics and Electronics, Christ (Deemed to be University), Bangalore, Karnataka 560029, India

ARTICLE INFO

Keywords:
Strontium aluminate
Phosphor
Plant cell imaging
Cytotoxicity
Phytotoxicity

ABSTRACT

This study explores the novel application of terbium-doped strontium aluminate nanoparticles for fluorescence imaging in plant cells. The study encompasses microwave assisted solid state synthesis as well as the structural and optical characterization of terbium-doped strontium aluminate nanophosphors, their toxicity studies in plant and animal cells and their use as a fluorescent dye for plant imaging. The X-ray diffraction pattern analysis, along with Rietveld refinement studies, show the formation of $SrAl_2O_4$ as a dominant crystalline phase. Photoluminescence investigations demonstrate green emission from Tb^{3+} transition levels. *In vitro* biocompatibility of terbium-doped strontium aluminate nanophosphors was studied using L929 fibroblast cells. The plant *Clitoria ternatea* was used to examine phytotoxicity. The samples' potential for bioimaging was further investigated. Our findings reveal improved growth of seedlings, positioning these nanoparticles as promising tools in plant-related research. This study advances our understanding of nanoparticle-plant interactions and holds potential for transformative applications in agriculture.

1. Introduction

The study of nanophosphors has been extensively conducted over several decades, primarily because of their capability to emit light and their potential applications in various technological domains (Li et al., 2016; Chiatti et al., 2021). Nanophosphors have significantly transformed fields such as displays(Ashwini et al., 2020), lighting devices (Ganesh Kumar et al., 2020), imaging (Li et al., 2022), and energy conversion (Niklasson and Granqvist, 1991).

A significant advancement occurred in research focused on developing nanophosphors with desirable properties when Matsuzawa et al. made a groundbreaking discovery in 1996 (Matsuzawa et al., 1996). This discovery involved the identification of $SrAl_2O_4$:Eu^{2+}, Dy^{3+}, which replaced the previously prevalent fluorescent sulfides and thus opened up new avenues for further investigation into strontium aluminates and other types of aluminates. Since this discovery, alkaline earth aluminates activated with rare earth elements have been at the forefront of scientific inquiry. In particular, the SrO-Al_2O_3 system has been the subject of extensive research due to its exceptionally long afterglow times and highly intense bright emission, which surpasses that of its counterparts(Rojas-Hernandez et al., 2018; Neenu Mary Thomas, 2023). The utilization of rare earth activators in these phosphors provides numerous advantages, such as high emission efficiency, the ability to control the emission profile, and the production of sharp emission lines (Gupta et al., 2021). Consequently, rare earth-activated phosphors are regarded as remarkably efficient materials, primarily due to their remarkable optoelectronic, biochemical, and thermal characteristics, all of which contribute to their environmentally friendly nature. In literature, the $SrAl_2O_4$ host has been doped mainly with europium and co-doped with dysprosium. Still, comparatively few works report doping of $SrAl_2O_4$ with other rare earth elements like Tb, Ce, Sm, etc. Understanding the ongoing processes within the material is crucial for enhancing the optical characteristics of the durable aluminate luminophores in various applications. Nonetheless, there is insufficient clarity regarding the intricacies of these processes, particularly regarding the nature and significance of the defects involved. Researchers have yet to

* Corresponding author at: Optoelectronic and Nanomaterials' Research Lab, Department of Physics, Union Christian College, Aluva, Ernakulam, Kerala 683102, India.
E-mail address: anilaei@gmail.com (E.I Anila).

https://doi.org/10.1016/j.plana.2024.100072
Received 5 February 2024; Received in revised form 29 March 2024; Accepted 11 April 2024
Available online 16 April 2024

elucidate these aspects fully (Vitola et al., 2019).

The materials derived from $SrAl_2O_4$ demonstrate significant potential in various practical applications. These applications encompass using $SrAl_2O_4$ materials in luminescent paints in multiple industries, including automotive, ink production, ceramics, and textile manufacturing. Additionally, these materials find utility in numerous technologies, such as lighting systems (Ju et al., 2013), sensors (Bisen and Sharma, 2016), and LEDs (Jamalaiah and Jayasimhadri, 2019), as well as in the advancement of security encoding technologies (Rojas-Hernandez et al., 2018). The versatility of $SrAl_2O_4$-based materials extends their impact to various domains. They promise to shape intelligent highways(Sharma et al., 2009) and enhance solar cell technology (Wang, 2016). This family of compounds were used in creation of white light emitting diodes (WLEDs) to fulfill general illumination requirements (Ganesh Kumar et al., 2020). Furthermore, $SrAl_2O_4$ materials demonstrate potential in fingerprint technology, counterfeiting prevention applications(Ashwini, 2021), nanobionics (Giraldo, 2014), and thermoluminescent dosimetry(Gingasu et al., 2019).

Fluorescence imaging has garnered increased attention as a non-invasive and cost-effective technique that permits real-time imaging. Challenges encountered in the field of fluorescence bioimaging encompass the photobleaching and phototoxicity of fluorescent dyes (Gupta et al., 2021). In this context, Strontium aluminate based nanophosphors offers superior advantages like high emission intensity and biocompatibility. Using strontium aluminate in bioimaging has been the subject of only a limited number of studies. The core-shell structures of $SrAl_2O_4$: Eu, Dy encapsulated within biocompatible silica have been documented by Catlayud. Additionally, the study has confirmed the material's cellular uptake, efficient light transmission, and potential for in vitro optical imaging through confocal fluorescence microscopy (Calatayud, 2022).

The investigation of the impact of nanoparticles on plant systems represents an emerging field of study (Dong, 2019). The interplay between nanoparticles and plant organisms is a complicated phenomenon and depends upon the characteristics of the nanoparticles and the botanical species under consideration (Azim, 2023). Nanoparticles, by virtue of their miniscule dimensions, possess the innate ability to be absorbed by the intricate network of plant roots, thereby infiltrating and permeating the very fabric of the plant's vascular system. Plants absorb nanoparticles and affect plant activities, but their complete mechanism is unknown (Wang, 2023). Nanoparticles have reported both positive and negative impacts on plants at various concentrations. Studies have been conducted on the impact various nanoparticles on plants and their phytotoxicity (Hischemöller et al., 2009; Lin and Xing, 2007; Li, 2016; Yadav et al., 2014; Lin, 2007; Shafqat et al., 2023). S. Azariah et al. reported multicolour carbon dots as a novel and vital bioimaging agent for both animal cell and plant bioimaging (Assariha and Alvandi, 2023). Baskar et al. conducted a comparative investigation on the phytotoxic impacts of metal oxide nanoparticles, including CuO, ZnO, and NiO, on *in-vitro* cultivated *Abelmoschus esculentus*(Baskar, 2021). Several studies investigating the effects of engineered nanoparticles have also been reported (Mathur and Chakraborty, 2023; Budhani et al., 2019; Li et al., 2023; Yang et al., 2017; Xin, 2023; Giri and Kumari, 2023; Gupta et al., 2023; Preetha et al., 2023; Kumar et al., 2023). Few articles revealed a significant decline in plant biomass and the inhibition of shoot and root development. Upon being exposed to plants, nanoparticles can infiltrate the root epidermis through the cell wall and cell membrane, utilizing both apoplastic and simplistic pathways (Ullah, 2020; Lee et al., 2013). The apoplastic pathway involves nutrient movement through cell walls and intercellular spaces, whereas the symplastic pathway involves nutrient movement through plant cells via plasmodesmata. Subsequently, these nanoparticles may progress towards the plant vascular bundle and eventually relocate to the leaves. Currently, there is a lack of research exploring the effects of strontium aluminate-based phosphors on plant systems. To our knowledge this is the first work reporting the interaction of superior strontium aluminate based nanophosphor with plant systems in tissue culture, with special significance to the phytotoxicity and investigating its scope as a fluorescent dye. The exceptional properties of strontium aluminate-based nanophosphors hold great promise in this field of study. Comprehending the uptake and transport mechanisms of nanoparticles in agricultural plants is essential for the effective design of nanoparticles tailored for agricultural applications.

The current work includes microwave assisted solid state synthesis of Tb doped strontium aluminate nanoparticles. The obtained nanoparticles were characterized using X-ray diffraction (XRD), Field Emission scanning electron microscopy (FESEM) and photoluminescence. The cytotoxicity of the samples was studied using an MTT assay in fibroblast L929 cells. The phytotoxicity of terbium doped strontium aluminate nanoparticles was studied in *Clitoria ternatea* plants grown in tissue culture. The changes in root and shoot lengths were studied for three weeks. The presence of fluorescence was confirmed using photographs of nanophosphor exposed plant under a UV lamp using a CCD camera. The *in vivo* imaging of plants was carried out using a fluorescence microscope.

Our results explore the growth promoting effects of Tb doped strontium aluminate nanophosphors in plants and attempt to study the scope of using these nanophosphors as a suitable imaging probe for plant systems.

2. Experimental

Materials: Precursor materials for the synthesis included aluminium oxide active (Al_2O_3; Merck; 99.99%), strontium carbonate ($SrCO_3$; Merck; 99.9%), and $TbN_2O_3.5\ H_2O$ (99.99%).

Synthesis of Tb-doped strontium aluminate nanoparticles: Microwave-assisted solid-state reaction was employed to synthesize Tb (4 at%) doped strontium aluminate ($SrAl_2O_4$: Tb^{3+}) nanoparticles. Stoichiometric ratios of starting materials were ground using mortar and pestle for 1 hour and placed in a microwave furnace (VB Ceramics) in a 25 mL crucible in the susceptor cavity. The target temperature of 1100^0 C was attained with a rise of 35^0 C/minute, and the sample was maintained at this temperature for 1 hr. After heating, the sample was allowed to cool down to room temperature naturally.

Characterization of Tb-doped strontium aluminate nanoparticles: X-ray diffractogram was recorded using PANalytical diffractometer (Cu- Kα radiation) in the 2θ range from 10^0 to 80^0 at scanning step size of 0.04^0. Field emission scanning electron microscope (FESEM) MIRA3 was used to analyze the morphology of the sample at a magnification of 150kx. The photoluminescence studies of the sample were conducted using a fluoromax 4 C spectrofluorometer (a 150 W xenon lamp as the source) at an excitation wavelength of 260 nm and emission range from 280 to 700 nm with a break in the region of second harmonics 500–530 nm.

Cytotoxicity assay of Tb-doped strontium aluminate nanoparticles: Viability assays were performed using L929 (Fibroblast) cells (procured from NCCS Pune) in Dulbecco's modified Eagle's medium (DMEM) supplemented with essential amino acids at 37 °C in a humidified CO_2 incubator. 96-well tissue culture plate seeded with 100 μL of the cell suspension (5×10^4 cells/well) in 10%(w/v) growth medium was placed in an incubator at 37ºC. Using a cyclomixer, the stock solution was prepared by weighing 1 mg of the sample and dissolving it in 1 mL DMEM. Five different concentrations of the nanoparticles, specifically 100 μg/mL, 50 μg/mL, 25 μg/mL, 12.5 μg/mL and 6.25 μg/mL were obtained by further dilution of stock solution. Subsequently, 100 μL of each concentration was meticulously introduced in triplicates to their corresponding wells, followed by incubation at a temperature of 37ºC within a controlled environment of 5% CO_2(w/v) for 24 hours. For comparative analysis, non-treated cells were maintained as control. The cells were permitted to proliferate for twenty-four hours. Microscopic observation was recorded as images taken using a tissue culture microscope (Olympus CKX41 with Optika Pro5 CCD camera) in inverted phase contrast mode. Cytotoxicity Assay was also carried out using the

MTT (dimethylthiazol-diphenyltetrazolium bromide) assay method. 15 mg of MTT (Sigma, M-5655) was reconstituted in 3 mL phosphate-buffered saline (PBS). After 24 hours of incubation, the sample content in wells was detached, and 30 μL of reconstituted MTT solution was included in control and test cell wells for formazan crystal formation. After the incubation period of 4 hours, the supernatant was separated, and 100 μL Dimethyl sulphoxide(DMSO, Sigma Aldrich) was supplemented to solubilize the formazan crystals. The optical density was measured using a microplate reader (Erba LisaScan EM) at a wavelength of 540 nm. The statistical data analysis was done using one way ANOVA.

Phytotoxicity analysis of Tb-doped strontium aluminate nanoparticles: For the *in vitro* plant tissue culture, *Clitoria ternatea* (common name Butterfly Pea) plants were identified, and seeds were aseptically collected. In a laminar flow hood, the surface sterilization procedure was conducted under a sterilized condition. The seeds were sterilized using 70% (w/v) ethanol for 30 seconds and then washed with sterile distilled water thrice. The seeds were then submerged into mercuric chloride (1% (w/v), 1 min) and detergent Tween-20 (0.05%(w/v)) (1 min). The seeds were rinsed at least three times with sterile distilled water, discarding all the treatment solutions. Murashige and Skoog (MS) medium (Murashige and Skoog, 1962) is prepared by mixing macronutrients, micronutrients, and vitamins solution. Medium is supplemented with 30 gm sugar and 1 mg/L gibberellic acid (GA3). By adding 1 M of sodium hydroxide (NaOH) pH was adjusted to pH 7.00. 7.5 gm/L agar was added and then stirred until it was completely dissolved. The solution was then heated in the microwave to dissolve the components and poured into tissue culture flasks. All the precisely labelled flasks (250 mL) were then placed in the autoclave and sterilized for 20 min at 121 °C. Further, terbium doped strontium aluminate nanophosphors were prepared and transferred to sterilized containers aseptically. Different concentrations (0, 1 mg/L, 2 mg/L, 3 mg/L, 4 mg/L, 5 mg/L) of nanophosphor were supplemented in the medium. After sterilization, the medium was allowed to cool, and surface sterilized *C. ternatea* seeds were aseptically inoculated. Flasks were incubated in a growth room set at 25 ± 1°C temperature, 60% relative humidity and 50 μmol/m^2/s photosynthetic photon flux density (using cool white LED lights) for 16 hours photoperiod after perfectly sealing with parafilm. Flasks were observed daily to assess nanoparticles' effect on plant growth. Control and nanophosphor supplemented flasks show seed sprouting one day after incubation; for the quantitative assessment of plant growth, root length and stem length were measured on completion of the first, second and third week. Nanoparticle-exposed whole plants and cross sections were further examined using a CCD camera under visible and UV light and a fluorescent microscope Nikon Ti-2 U Eclipse with 20x magnification.

3. Results and discussions

The XRD pattern of the sample confirms the presence of strontium aluminate phases, dominant phase being monoclinic $SrAl_2O_4$ (JCPDS No. 34–0379) along with minor phase corresponding to cubic $Sr_3Al_2O_6$ (JCPDS No.24- 1187) as shown in Fig. 1. The average crystallite size is found out using Scherrer equation, and is obtained as 22 nm and 18 nm for the for $SrAl_2O_4$ and $Sr_3Al_2O_6$ phases respectively. Rietveld refinement of the XRD data was carried out using Full Prof software (Rodriguez-Carvajal, 1990). The data was fitted with Thompson-Cox-Hastings pseudo-Voigt (Axial divergence asymmetry) peak function and obtained a chi^2 value 6.22, the phase fraction 67.17% of $SrAl_2O_4$ and 32.83% of $Sr_3Al_2O_6$ phase were obtained from the results.

Fig. 2(a) presents FESEM images of the sample exhibiting terbium-doped strontium aluminate nanoparticles. The particles are found to be nearly spherical grain like morphology, along with agglomerated plate like structures. The composition of the sample was assessed using Energy Dispersive Spectroscopy (EDS), revealing the existence of strontium (Sr), aluminum (Al), oxygen (O), and terbium (Tb) elements. The EDX maps demonstrate the uniform dispersion of these distinct atoms within the sample, illustrating the effective integration of doped Tb ions into the host matrix (Fig. 2(b)). The particle size distribution was assessed using ImageJ software, considering spherical grain like structures only and the average particle size is obtained to be 40 nm. Size distribution of spherical particles is obtained as in fig. S1(supplementary file).

Fig. 3(a), illustrates the photoluminescence (PL) emission spectrum of terbium doped strontium aluminate nanoparticles excited at 260 nm. The emission spectrum possesses distinct satellite peaks at 379 nm, 419 nm, 437 nm, 468 nm, and 473 nm corresponds to transition between Tb^{3+} energy levels, on a broad peak spanning from 300 nm to 500 nm which is supposed to be due to point defects in the crystal (Thomas et al., 2020). The intense peaks in the blue region at 379, 419, 437, and 468 nm, are caused by the $^5D_3 \rightarrow {}^7F_j$ (j=6,5,4,3) transitions (Zhai and Huang, 2017; Su et al., 2022; Jamalaiah and Madhu, 2020; Page et al., 2008; Mindru and Gingasu, 2017; Mindru and Gingasu, 2017). The transition from the $^5D_4$ state to the $^7F_6$ state in the terbium ion leads to the occurrence of an emission peak at a wavelength of 488 nm (Li et al., 2016). The remarkable intense green emissions centered at 542 nm and 551 nm corresponds to the emission originating from $^5D_4 \rightarrow {}^7F_5$ transition in Tb^{3+} energy levels, this doublet is attributed to the existence of two types of sites for the Tb^{3+} ions substitution in the host lattice (Kumar et al., 2014; Annadurai et al., 2016). Beyond green region, two mild peaks are exhibited at 583 nm and at 623 nm which is attributed to $^5D_4 \rightarrow {}^7F_j$(j=3,4) transitions (Safeera and Anila, 2018).

The chromaticity diagram offers a graphical representation

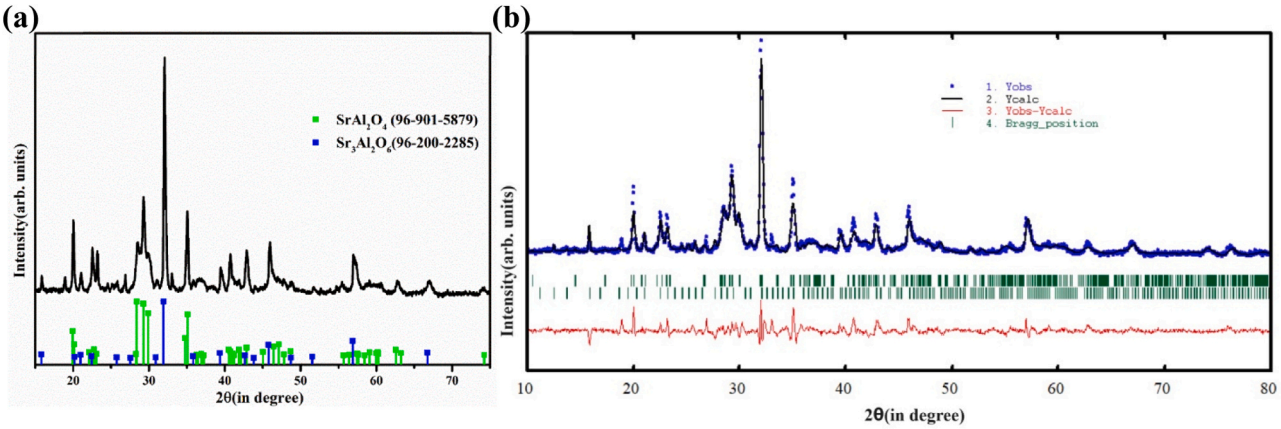

Fig. 1. (a) X-ray diffraction pattern of Tb^{3+} doped strontium aluminate nanoparticles along with standards peaks of phases present. (b) Rietveld refinement plot of Tb doped strontium aluminate nanoparticles.

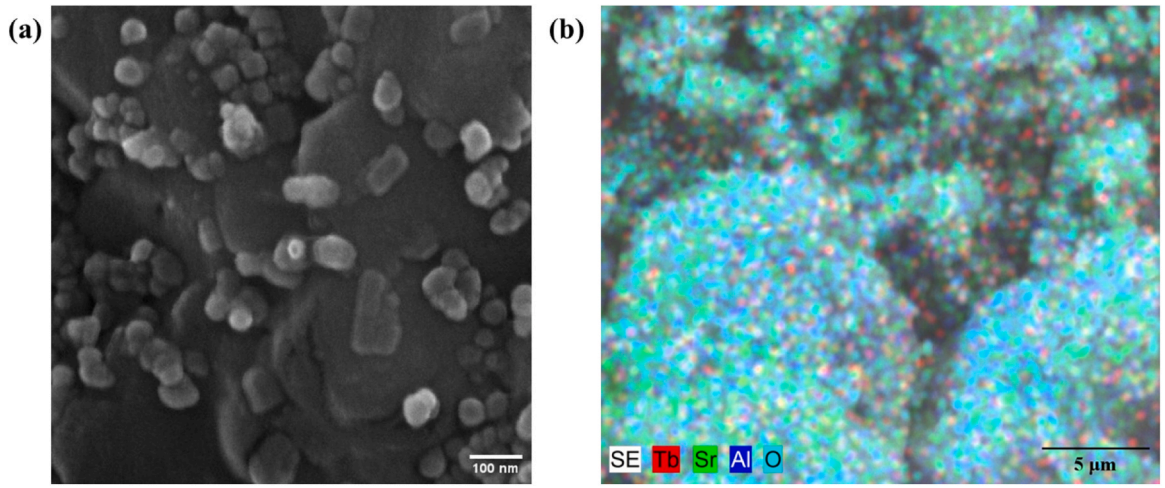

Fig. 2. FESEM images(150 Kx) and EDS mapping (a) FESEM image of Tb doped strontium aluminate (b) the EDS mappings of elements Tb, Sr, Al and O.

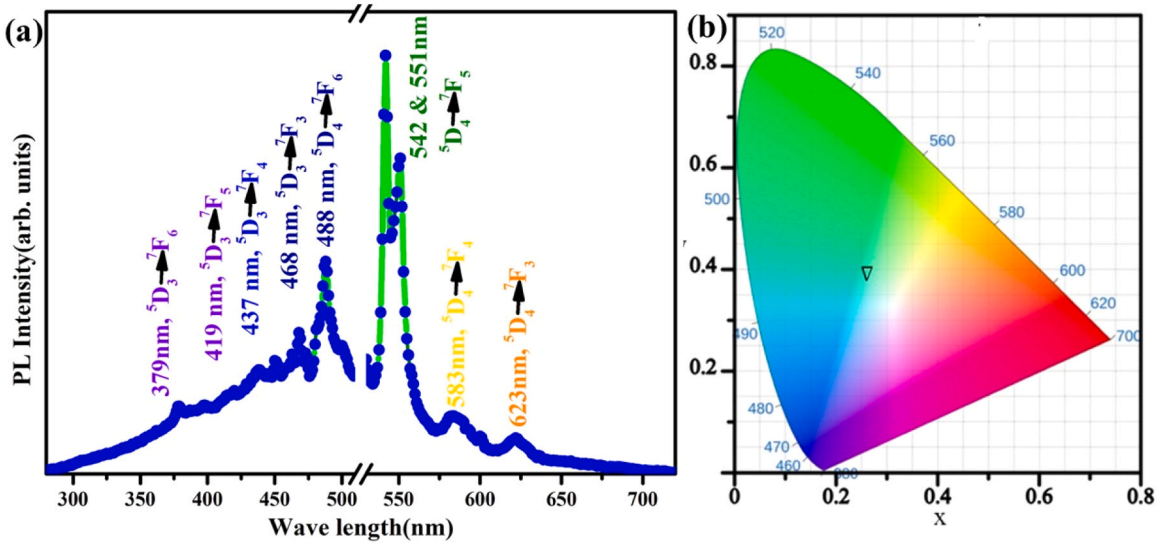

Fig. 3. (a) PL Spectrum of terbium doped strontium aluminate monitored at 260 nm excitation (b) CIE coordinates depicted on 1931 chart where X = 0.26 and Y = 0.39 of Tb (4 at%) doped strontium aluminate phosphor.

facilitating comprehension of color characteristics. The light's color is denoted by two parameters, the x and y chromaticity coordinates, derived from the tristimulus values X, Y, and Z, which are determined by convolution integrals of the spectral power distribution. The Commission Internationale de l'Eclairage (CIE) chromaticity coordinates for the sample is found to be (0.26, 0.39), as shown in CIE chromaticity diagram Fig. 3(b),which depicts the green emission from the nanophosphor.

I*n vitro* animal tissue cultures, was used to investigate the effects of terbium-doped strontium nanophosphors on cell viability and cytotoxicity in animal cells. Fig. 4 and Fig. 5 show the in vitro cytotoxicity of Tb-doped strontium aluminate nanophosphors, as measured by the MTT assay on L929 fibroblast cells. The survival rate of cells after 24 hours of incubation with different concentrations of nanoparticles was evaluated. A microplate reader evaluated the absorbance values at 540 nm. The percentage of viability of cells was assessed using the obtained optical density (OD), using the equation

$$\%\text{cell viability} = \frac{\text{Mean OD of sample}}{\text{Mean OD of control}} \text{X}100$$

IC_{50} value of the sample was found to be 162.122 µg/mL. The viability of the L929 cells was found to be more than 70% for all considered concentrations, which is in agreement with the cut-off for cytotoxicity as suggested by ISO 10993–5: 2009 (Biological evaluation of medical devices part-5: tests for in-vitro cytotoxicity)(Rekha and Anila, 2019; Nath et al., 2023) and thus demonstrates that Tb doped strontium aluminate nanoparticles are biocompatible at a varied range of concentrations(Table S1, Supplementary file).

The Tb doped strontium aluminate nanophosphors were incorporated in the plant tissue culture medium of *Clitoria ternatea* to study its effect on plant growth. The influence of nanoparticle exposure in plant is interpreted by analyzing the rate of seedling elongation. The experiment involved recording changes in root and stem lengths of *Clitoria ternatea* seeds exposed to diverse concentrations of nanoparticles on completion of week 1, 2 and 3. These measurements were taken to assess the potential phytotoxic and growth promoting effects of the nanoparticles. Fig. 6, Table S2 and Table S3(supplementary file) illustrates the changes observed in root and stem elongation upon exposure to terbium-doped strontium aluminate nanoparticles. Our results showed that these nanoparticles do not have any phytotoxicity during seedling growth. Instead it exhibited a growth promoting property evident enhanced root ant shoot growth in the terbium doped strontium aluminate nanoparticles treated *Clitoria ternatea* seeds in *in vitro* culture.

Seed germination and seedling establishment are the crucial stage of plant growth, which affect plant growth, yield and quality. Our results

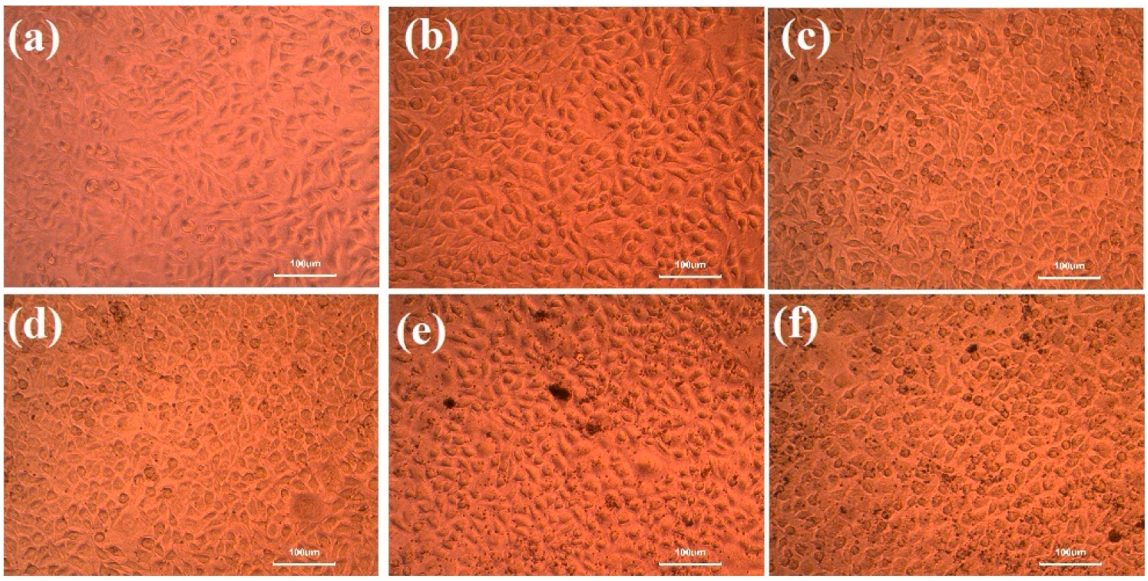

Fig. 4. Microscopic photographs of L929 cells exposed to different levels of terbium doped strontium aluminate. (a) control (b) 6.25 μg/mL (c) 12.5 μg/mL (d) 25 μg/mL (e) 50 and (f) 100 μg/mL.

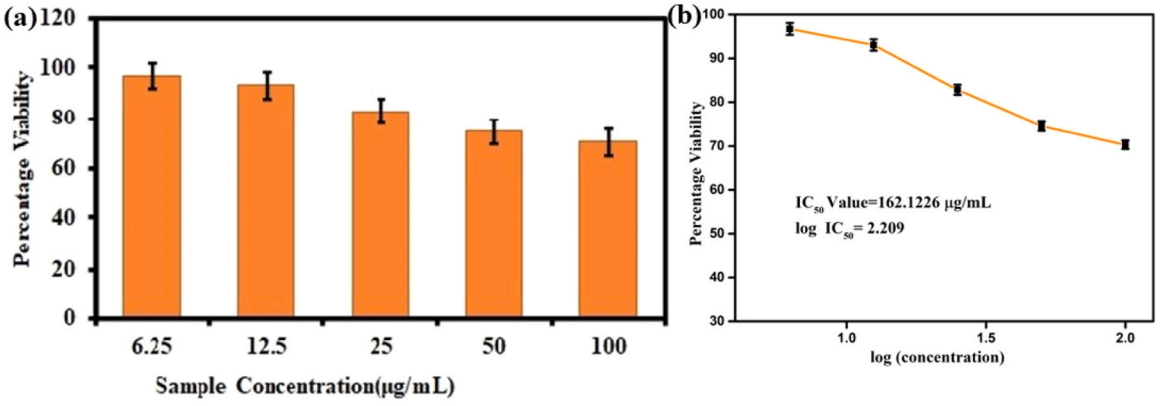

Fig. 5. Analysis results of in-vitro cytotoxicity of Tb doped strontium aluminate nanophosphors, using MTT assay. (a) Graph showing percentage viability versus concentration of nanoparticles and (b) graph for finding IC50 value for nanoparticles.

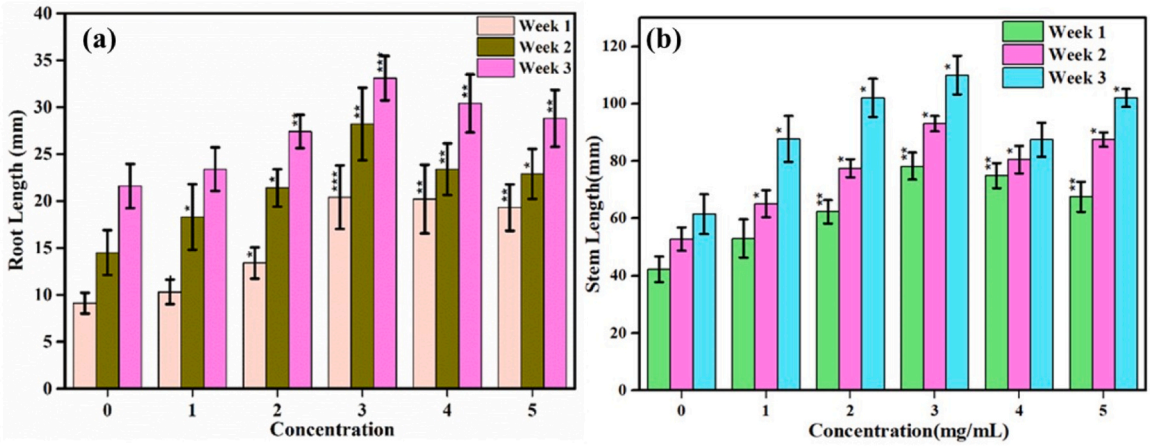

Fig. 6. Variation of (a) the length of root (b) length of stem of *Clitoria ternatea* seeds grown in different concentrations of terbium doped strontium aluminate nanoparticles after week 1, week 2 and week 3. Error bars correspond to standard deviation. * Mean values were significantly different when compared with the control group ($P < 0.05$); * * Mean values were significantly different when compared with the control group ($P < 0.01$); *** Mean values were significantly different when compared with the control group ($P < 0.001$).

showed that terbium doped strontium aluminate nanoparticles have no adverse effect on platelet growth. Quantitative analysis of plant growth parameters points out that the Tb doped nanophosphor showed a statistically significantly improvement in the early development of the plant. It is found that enhanced growth of root as well as stem is more pronounced for sample concentration of 3 mg/mL. The nanophosphor induced significant increase in the seed germination rates can be attributed to the small size of the particles. It is reported that the nanoparticles can penetrate the seed and induce germination. The beneficial effect of nanoparticles on seedling growth can be due to their ability to increase water absorption, alter bioavailability, efficiently utilize nutrients, enhance nitrate reductase activity, and increased resistance to biotic and abiotic stress (Zheng et al., 2005; Changmei et al., 2002; Munir, 2018; Zhao, 2020).

To study the uptake and translocation of terbium-doped strontium aluminate nanoparticles, digital images of the control plant and nanophosphor exposed plant were taken using a CCD camera under visible and UV light as shown in Fig. 7. It is shown that control and nanoparticle-exposed plants are visible under visible light. When plants are illuminated only with UV light, the control plant is not visible, but regions of nanoparticles exposed plants can be seen with florescence. It can be inferred from Fig. 7 that plants uptake terbium-doped strontium aluminate nanoparticles in the medium and translocate it through the root and stem.

The presence of nanoparticles in the stem of plant confirmed that the terbium doped strontium aluminate nanoparticles were able to enter and translocate through the vascular system of the developing plantlet. The nanophosphors may aid its absorption and subsequent transportation to the xylem of the root (Parkinson et al., 2022). Due to its small size, less than 25 nm, Tb doped strontium aluminate nanophosphors can be internalized by the root cells through endocytosis (Ma and Yan, 2018). The inorganic nature, small size and the neutral charge will allow the nanoparticles to be transported through the extracellular space (Miralles, 2012). Further, the unmatured epidermis and exodermis of the developing seedling of *Clitoria ternatea* can permeate nanoparticles to the central column or xylem of the root (Enstone et al., 2002).

To confirm the uptake of nanophosphors by plants, fluorescent microscope imaging of cross sections of root and stem was taken Fig. 8. The images show the successful absorption and transportation of fluorescent nanoparticles through vascular tissue of the living plant. The cross-sections of root and shoot of plants grown in nanophosphor-containing medium exhibit bright green emission in xylem and phloem regions on exciting in the wavelength range 465 nm to 495 nm. Fluorescence inferred that Tb doped nanophosphors move extracellularly through the tissues until they reach the xylem (Dong, 2019).

In fluorescence imaging of the root cross sections, terbium doped strontium aluminate nanoparticle localization was observed in the Casparian strip and around the vascular system. This is due to the transportation of the nanoparticles through the epidermis to the endothelium, then they will be partially blocked by the developing Casparian strip. Terbium doped strontium aluminate nanoparticle reaching the vascular system will be transport through the xylem (Schwab et al., 2016; Li et al., 2020). The nanoparticle is distributed in a concentration depended manner along the developing plant. Hence it is evident that the terbium doped strontium aluminate nanoparticles is mostly transported through the exoplast pathway, instead of symplast pathway.

Our results indicate the possible use of Tb doped strontium aluminate nanoparticles as a fluorescent *in vivo* probe for live plant imaging due to its photoluminescence, biocompatibility, low cytotoxicity, chemical/physical stability and phyto-compatibility. Most fluorescent dyes available in the market are synthetic organic compounds, which cannot be used for live-cell imaging due to their toxicity (Bouccara et al., 2015). Unlike the organic fluorophores, Tb doped nanophosphor is actively transported into the growing plants and incorporated into roots and shoots without affecting plant growth. Nanophosphor-incorporated live plants can be excited *in vivo* with deep penetration lasers. Hence, this nanophosphor can be used for non-invasive long-term plant cell imaging, which is significant for investigating biological structures, processes, pathological pathways, and therapeutic effects over long periods. Further, the sample enables the direct fluorescent visualization and imaging of plants without any staining, and it can also be used along with other fluorescent and non-fluorescent staining procedures. Tb-doped strontium aluminate nanoparticles presents additional potential in areas such as bioimaging, biosensing, precise nanoparticle delivery, and genetic modification (Dong, 2019).

The unique properties that nanoparticles make it difficult to predict the possible environmental and health risks associated with release of nanoparticles to the environment. Strontium aluminate, the host used in the present study, is chemically inert and biocompatible (Adel et al., 2022; Hopkins, 2023). Occupational Safety and Health Administration (OSHA) lists strontium aluminates as non-toxic, and non-flammable (Hopkins, 2023). Strontium aluminates doped with rare-earth elements are being used in various applications including emergency signage, textile printing, displays and biomedical imaging. But introduction of Tb doped strontium aluminate nanoparticles in complex systems such as soils may have unidentified fate and reactivity. Further investigation to assess the health and environmental effects of the nanoparticle is necessary.

4. Conclusions

In conclusion, bright green light emitting Tb doped strontium aluminate nanophosphors were synthesized by facile one step microwave assisted solid state reaction. The structural and optical characterisation of the nanophosphor was carried out. Photoluminescence emission spectrum confirmed high intense doublet emission at 542 nm and 551 nm corresponding to Tb^{3+} $^5D_4 \rightarrow {}^7F_5$ transition. The cytotoxicity assay of the nanophosphors on L929 fibroblast cells confirmed the biocompatibility of the sample with an IC50 value 162.122 μg/mL. The influence of nanophosphors in plants were explored by incorporating it in tissue culture of Clitoria ternatea seeds. It is found that Tb doped nanophosphor is actively transported into the growing plants and incorporated into roots and shoots without any adverse effect on plant growth, but enhances the growth when used in an optimum quantity. The sample enables the direct fluorescent visualization and imaging of plants without any staining, thereby indicating its potential as an imaging probe.

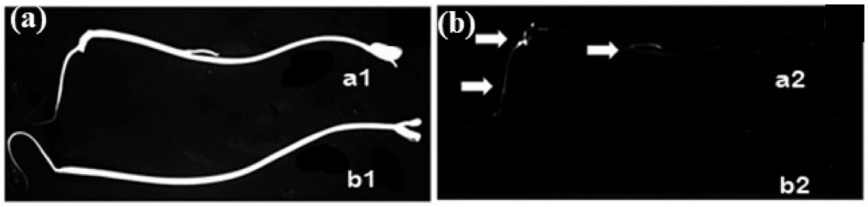

Fig. 7. Image of Tb doped strontium aluminnate exposed plant (a2) and Control(b2) in CCD camera under (a) normal light (b) UV light.

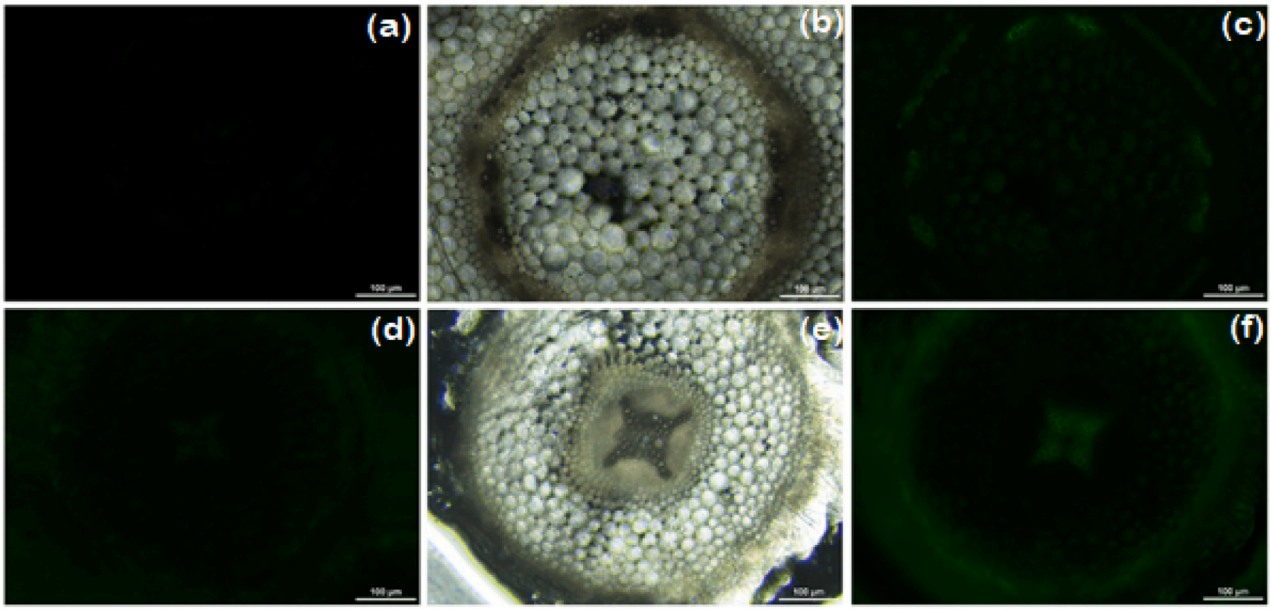

Fig. 8. Cross-sections of *Clitoria ternatea* Linn. imaged using a fluorescent/phase-contrast microscope. (a) fluorescent image of control shoot (b) brightfield image of shoot of plants grown in Terbium doped nanophosphor containing medium (c) fluorescent image of shoot of plant grown in nanophosphor containing medium (d) fluorescent image of control root, (e) brightfield image of root of plants grown in terbium doped strontium aluminate containing medium (f) fluorescent image of root of plants grown in nanophosphor containing medium.

CRediT authorship contribution statement

Anila E I: Writing – review & editing, Validation, Supervision, Methodology, Conceptualization. **M O Viji:** Validation, Investigation, Formal analysis, Data curation. **Naijil George:** Visualization, Validation, Methodology, Investigation, Data curation. **Neenu Mary Thomas:** Writing – review & editing, Writing – original draft, Methodology, Investigation, Formal analysis, Data curation, Conceptualization.

Declaration of Competing Interest

The authors declare that they have no known competing financial interests or personal relationships that could have appeared to influence the work reported in this paper.

Data availability

Data will be made available on request.

Acknowledgement

The authors acknowledge the Science and Engineering Research Board (SERB), Department of Science and Technology (DST), Government of India for funding through a major project (EMR/2017/002882). EIA thanks Christ University for the research grants (SMSS-2218 and SMSS-2329).

Appendix A. Supporting information

Supplementary data associated with this article can be found in the online version at doi:10.1016/j.plana.2024.100072.

References

Adel, Sherif, Hashimoto, Kentaro, Kawashima, Nobuyuki, Wada, Takahiro, Uo, Motohiro, Okiji, Takashi, 2022. Biocompatibility and pro-mineralisation effect of tristrontium aluminate cement for endodontic use. ISSN 1991-7902 J. Dent. Sci. Volume 17 (Issue 3), 1193–1200. https://doi.org/10.1016/j.jds.2021.12.018.

Annadurai, G., Jayachandiran, M., Kennedy, S.M.M., Sivakumar, V., 2016. Synthesis and photoluminescence properties of $Ba_2CaZn_2Si_6O_{17}$:Tb^{3+} green phosphor. Mater. Sci. Eng. B Solid-State Mater. Adv. Technol. vol. 208, 47–52. https://doi.org/10.1016/j.mseb.2016.02.008.

Ashwini, K.R., et al., 2021. Green emitting $SrAl_2O_4$:Tb^{3+} nano-powders for forensic, anti-counterfeiting and optoelectronic devices. Inorg. Chem. Commun. vol. 130 (February), 108665 https://doi.org/10.1016/j.inoche.2021.108665.

Ashwini, K.R., Premkumar, H.B., Darshan, G.P., Basavaraj, R.B., Nagabhushana, H., Daruka Prasad, B., 2020. Near UV-light excitable $SrAl_2O_4$:Eu^{3+} nanophosphors for display device applications. J. Sci. Adv. Mater. Devices vol. 5 (1), 111–118. https://doi.org/10.1016/j.jsamd.2020.02.003.

Assariha, S., Alvandi, N., et al., 2023. Bioinspired multicolour carbon dots: comprehensive cytotoxicity, phytotoxicity, and bioimaging in animal cells and plants. Luminescence vol. 38 (5), 554.

Azim, Zeba, et al., 2023. A review summarising uptake, translocation and accumulation of nanoparticles within the plants: current status and future prospectus. J. Plant Biochem. Biotechnol. vol. 32 (2), 211–224. https://doi.org/10.1007/s13562-022-00800-6.

Baskar, Venkidasamy, et al., 2021. A comparative study of phytotoxic effects of metal oxide (CuO, ZnO and NiO) nanoparticles on in-vitro grown Abelmoschus esculentus. Plant Biosyst. - Int. J. Deal. all Asp. Plant Biol. 155 (2), 374–383. https://doi.org/10.1080/11263504.2020.1753843.

Bisen, D.P., Sharma, R., 2016. Mechanoluminescence properties of $SrAl_2O_4$:Eu^{2+} phosphor by combustion synthesis. Luminescence vol. 31 (2), 394–400. https://doi.org/10.1002/bio.2972.

Bouccara, S., Sitbon, G., Fragola, A., Loriette, V., Lequeux, N., Pons, T., 2015. Enhancing fluorescence in vivo imaging using inorganic nanoprobes. Curr. Opin. Biotechnol. vol. 34, 65–72. https://doi.org/10.1016/j.copbio.2014.11.018.

Budhani, S., Egboluche, N.P., Arslan, Z., Yu, H., Deng, H., 2019. Phytotoxic effect of silver nanoparticles on seed germination and growth of terrestrial plants. J. Environ. Sci. Health C. Environ. Carcinog. Ecotoxicol. Rev. 37 (4), 330–355. https://doi.org/10.1080/10590501.2019.1676600. Epub 2019 Oct 29. PMID: 31661365; PMCID: PMC7773158.

Calatayud, D.G., et al., 2022. Biocompatible probes based on rare-earth doped strontium aluminates with long-lasting phosphorescent properties for in vitro optical imaging. Int. J. Mol. Sci. vol. 23 (6) https://doi.org/10.3390/ijms23063410.

Changmei, L., Chaoying, Z., Junqiang, W., Guorong, W., Mingxuan, T., 2002. Research of the effect of nanometer materials on germination and growth enhancement of Glycine max and its mechanism. Soybean Sci. vol. 21 (3), 168–171 [Online]. Available: ⟨http://europepmc.org/abstract/CBA/371541⟩.

Chiatti, C., Fabiani, C., Pisello, A.L., 2021. Long Persistent Luminescence: a road map toward promising future developments in energy and environmental science. Annu. Rev. Mater. Res. vol. 51, 409–433. https://doi.org/10.1146/annurev-matsci-091520-011838.

Dong, R., et al., 2019. Recent developments in luminescent nanoparticles for plant imaging and photosynthesis. J. Rare Earths vol. 37 (9), 903–915. https://doi.org/10.1016/j.jre.2019.04.001.

Enstone, D.E., Peterson, C.A., Ma, F., 2002. Root endodermis and exodermis: structure, function, and responses to the environment. J. Plant Growth Regul. 21, 335–351. https://doi.org/10.1007/s00344-003-0002-2.

Ganesh Kumar, K., Balaji Bhargav, P., Aravinth, K., Arumugam, R., Ramasamy, P., 2020. Dysprosium activated strontium aluminate phosphor: a potential candidate for WLED applications. " *J. Lumin.* vol. 223, 117126 https://doi.org/10.1016/j.jlumin.2020.117126.

Ganesh Kumar, K., Balaji Bhargav, P., Aravinth, K., Arumugam, R., Ramasamy, P., 2020. Dysprosium activated strontium aluminate phosphor: a potential candidate for WLED applications. J. Lumin. vol. 223 (September 2019), 117126 https://doi.org/10.1016/j.jlumin.2020.117126.

Gingasu, D., Mindru, I., Ianculescu, A., Preda, S., Negrila, C., Secu, M., 2019. Photoluminescence and thermoluminescence properties of the $Sr_3Al_2O_6$:Eu^{3+}/Eu^{2+}, Tb^{3+} persistent phosphor. J. Lumin. vol. 214, 116540 https://doi.org/10.1016/j.jlumin.2019.116540.

Giraldo, J.P., et al., 2014. Plant nanobionics approach to augment photosynthesis and biochemical sensing. Nat. Mater. vol. 13 (4), 400–408. https://doi.org/10.1038/nmat3890.

Giri, Ved Prakash, Kumari, Madhuree, 2023. Microbial approaches in fabrication of nanoscale materials effectively enhance the antimicrobial and crop protection potential–A review. ISSN 2773-1111 Plant Nano Biol. Volume 3, 100027. https://doi.org/10.1016/j.plana.2023.100027.

Gupta, Anmol, Rayeen, Fareha, Mishra, Richa, Tripathi, Manikant, Pathak, Neelam, 2023. Nanotechnology applications in sustainable agriculture: an emerging eco-friendly approach. ISSN 2773-1111 Plant Nano Biol. Volume 4, 100033. https://doi.org/10.1016/j.plana.2023.100033.

Gupta, I., Singh, S., Bhagwan, S., Singh, D., 2021. Rare earth (RE) doped phosphors and their emerging applications: a review. Ceram. Int. vol. 47 (14), 19282–19303. https://doi.org/10.1016/j.ceramint.2021.03.308.

Gupta, S.K., Sudarshan, K., Kadam, R.M., 2021. Optical nanomaterials with focus on rare earth doped oxide: a review. Mater. Today Commun. vol. 27 (March), 102277 https://doi.org/10.1016/j.mtcomm.2021.102277.

Hischemöller, A., Nordmann, J., Ptacek, P., Mummenhoff, K., Haase, M., 2009. "In-vivo imaging of the uptake of upconversion nanoparticles by plant roots. J. Biomed. Nanotechnol. vol. 5 (3), 278–284. https://doi.org/10.1166/jbn.2009.1032.

Hopkins, Scarlet L., et al., 2023. Preparation of a low-cost fingerprint powder that harnesses white light to emit long-lived phosphorescence. Sci. Justice.: J. Forensic Sci. Soc. vol. 63 (4), 500–508. https://doi.org/10.1016/j.scijus.2023.04.013.

Jamalaiah, B.C., Jayasimhadri, M., 2019. Tunable luminescence properties of $SrAl_2O_4$: Eu^{3+} phosphors for LED applications. J. Mol. Struct. vol. 1178, 394–400. https://doi.org/10.1016/j.molstruc.2018.10.060.

Jamalaiah, B.C., Madhu, N., 2020. Luminescence properties of $SrAl_2O_4$: Tb^{3+}/ Bi^{3+} nanophosphors for photonic applications. ISSN 0022-2860 J. Mol. Struct. Volume 1205, 127599. https://doi.org/10.1016/j.molstruc.2019.127599.

Ju, H., Liu, J., Wang, B., Tao, X., Ma, Y., Xu, S., 2013. Bi 3+-doped $Sr_3Al_2O_6$: an unusual color-tunable phosphor for solid state lighting. Ceram. Int. vol. 39 (1), 857–860. https://doi.org/10.1016/j.ceramint.2012.05.106.

Kumar, Subodh, Dwivedi, Archana, Kumar Pandey, Alok, Vajpayee, Poornima, 2023. TiO_2 nanoparticles alter nutrients acquisition, growth, biomacromolecules, oil composition and modulate antioxidant defense system in Mentha arvensis L. ISSN 2773-1111 Plant Nano Biol. Volume 3, 100029. https://doi.org/10.1016/j.plana.2023.100029.

Kumar, R.S., Ponnusamy, V., Jose, M.T., Sivakumar, V., 2014. Synthesis and photoluminescence studies on $YAl_3(BO_3)_4$:Tb^{3+} phosphor. EPJ Appl. Phys. vol. 68 (3), 1–7. https://doi.org/10.1051/epjap/2014140244.

Lee, S., Kim, S., Kim, S., et al., 2013. Assessment of phytotoxicity of ZnO NPs on a medicinal plant, Fagopyrum esculentum. Environ. Sci. Pollut. Res 20, 848–854. https://doi.org/10.1007/s11356-012-1069-8.

Li, W., et al., 2016. Phytotoxicity, uptake, and translocation of fluorescent carbon dots in mung bean plants. ACS Appl. Mater. Interfaces vol. 8 (31), 19939–19945. https://doi.org/10.1021/acsami.6b07268.

Li, Y., Gecevicius, M., Qiu, J., 2016. Long persistent phosphors - From fundamentals to applications. Chem. Soc. Rev. vol. 45 (8), 2090–2136. https://doi.org/10.1039/c5cs00582e.

Li, W., Kaminski Schierle, G.S., Lei, B., Liu, Y., Kaminski, C.F., 2022. Fluorescent Nanoparticles for Super-Resolution Imaging. Chem. Rev. vol. 122 (15), 12495–12543. https://doi.org/10.1021/acs.chemrev.2c00050.

Li, Kai, Liang, Sisi, Shang, Mengmeng, Lian, Hongzhou, Lin, Jun, 2016. Photoluminescence and Energy Transfer Properties with Y+SiO_4 Substituting Ba+PO_4 in $Ba_3Y(PO_4)_3$:Ce^{3+}/Tb^{3+}, Tb^{3+}/Eu^{3+} Phosphors for w-LEDs. Inorg. Chem. 55 (15), 7593–7604. https://doi.org/10.1021/acs.inorgchem.6b01040.

Li, L., Luo, Y., Li, R., et al., 2020. Effective uptake of submicrometre plastics by crop plants via a crack-entry mode. Nat. Sustain 3, 929–937. https://doi.org/10.1038/s41893-020-0567-9.

Li, Ziqian, Yan, Wende, Li, Yong, et al., 2023. Particle Size Determines the Phytotoxicity of ZnO Nanoparticles in Rice (Oryza sativa L.) Revealed by Spatial Imaging Techniques. Environ. Sci. Technol. 57 (36), 13356–13365. https://doi.org/10.1021/acs.est.3c03821.

Lin, Daohui, et al., 2007. Phytotoxicity of nanoparticles: inhibition of seed germination and root growth. ISSN 0269-7491 Environ. Pollut. Volume 150 (Issue 2), 243–250. https://doi.org/10.1016/j.envpol.2007.01.016.

Lin, D., Xing, B., 2007. Phytotoxicity of nanoparticles: inhibition of seed germination and root growth. Environ. Pollut. vol. 150 (2), 243–250. https://doi.org/10.1016/j.envpol.2007.01.016.

Ma, Xingmao, Yan, Jun, 2018. Plant uptake and accumulation of engineered metallic nanoparticles from lab to field conditions. ISSN 2468-5844 Curr. Opin. Environ. Sci. Health Volume 6, 16–20. https://doi.org/10.1016/j.coesh.2018.07.008.

Mathur, Piyush, Chakraborty, Rakhi, et al., 2023. Engineered nanoparticles in plant growth: phytotoxicity concerns and the strategies for their attenuation. ISSN 0981-9428 Plant Physiol. Biochem. Volume 199, 107721. https://doi.org/10.1016/j.plaphy.2023.107721.

Matsuzawa, T., Aoki, Y., Takeuchi, N., Murayama, Y., 1996. A new long phosphorescent phosphor with high brightness, $SrAl_2O_4$:Eu^{2+}, Dy^{3+},". J. Electrochem. Soc. vol. 143 (5), 4–7.

Mindru, Ioana, Gingasu, Dana, et al., 2017. Tb+-doped alkaline-earth aluminates: synthesis, characterization and optical properties. ISSN 0025-5408 Mater. Res. Bull. Volume 85, 240–248. https://doi.org/10.1016/j.materresbull.2016.09.024.

Mindru, Ioana, Gingasu, Dana, et al., 2017. Structural and optical properties of un-doped and doped $Sr_3Al_2O_6$ obtained through the tartarate precursor method. ISSN 0272-8842 Ceram. Int. Volume 43 (Issue 18), 16668–16675. https://doi.org/10.1016/j.ceramint.2017.09.057.

Miralles, Pola, et al., 2012. Toxicity, uptake, and translocation of engineered nanomaterials in vascular plants. Environ. Sci. Technol. vol. 46 (17), 9224–9239. https://doi.org/10.1021/es202995d.

Munir, T., et al., 2018. Effect of zinc oxide nanoparticles on the growth and Zn uptake in wheat (Triticum aestivum L.) by seed priming method. Dig. J. Nanomater. Biostruct. vol. 13, 315–323.

Murashige, T., Skoog, F., 1962. A revised medium for rapid growth and bio assays with tobacco tissue cultures. Physiol. Plant. vol. 15 (3), 473–497. https://doi.org/10.1111/j.1399-3054.1962.tb08052.x.

Nath, Soorya G., Jose, Jiya, Bins, K.C., Bhat, Sarita G., Anila, E.I., 2023. Monoclinic yttrium oxide quantum dots surface modified by biotin for bioimaging applications. ISSN 2468-0230 Surf. Interfaces Volume 40, 103112. https://doi.org/10.1016/j.surfin.2023.103112.

Neenu Mary Thomas, E.I.A., 2023. Synthesis and characterisation of $SrAl_2O_4$: Eu^{3+} orange-red emitting nanoparticles. J. Fluoresc. vol. 407, 3808–3812.

Niklasson, G.A., Granqvist, C.G., 1991. Selectively solar-absorbing surface coatings: optical properties and degradation. Mater. Sci. Sol. Energy Convers. Syst. 70–105. https://doi.org/10.1016/b978-0-08-040937-5.50008-5.

Page, Pallavi, Ghildiyal, Rahul, Murthy, K.V.R., 2008. Photoluminescence and thermoluminescence properties of $Sr_3Al_2O_6$:Tb^{3+}. ISSN 0025-5408 Mater. Res. Bull. Volume 43 (Issue 2), 353–360. https://doi.org/10.1016/j.materresbull.2007.03.001.

Parkinson, S.J., Tungsirisurp, S., Joshi, C., Richmond, B.L., Gifford, M.L., Sikder, A., Lynch, I., O'Reilly, R.K., Napier, R.M., 2022. Polymer nanoparticles pass the plant interface. Nat. Commun. 13, 7385.

Preetha, Jaganathan Sakthi Yazhini, Sriram, Duraisampath, Premasudha, Paramasivam, Pudake, Ramesh Namdeo, Arun, Muthukrishnan, 2023. Cerium oxide as a nanozyme for plant abiotic stress tolerance: an overview of the mechanisms. ISSN 2773-1111 Plant Nano Biol. Volume 6, 100049. https://doi.org/10.1016/j.plana.2023.100049.

Rekha, S., Anila, E.I., 2019. In vitro cytotoxicity studies of surface modified CaS nanoparticles on L929 cell lines using MTT assay. Mater. Lett. vol. 236, 637–639. https://doi.org/10.1016/j.matlet.2018.11.009.

J. Rodriguez-Carvajal, "Fullprof: A Program for Rietveld Refinement and Pattern Matching Analysis," Abstract of the Satellite Meeting on Powder Diffraction of the XV Congress of the IUCr, Toulouse, France, 1990, p. 127.

Rojas-Hernandez, R.E., Rubio-Marcos, F., Rodriguez, M.Á., Fernandez, J.F., 2018. Long lasting phosphors: $SrAl_2O_4$:Eu, Dy as the most studied material. Renew. Sustain. Energy Rev. vol. 81 (June), 2759–2770. https://doi.org/10.1016/j.rser.2017.06.081.

Safeera, T.A., Anila, E.I., 2018. Wet chemical approach for the low temperature synthesis of $ZnGa_2O_4$:Tb^{3+} quantum dots with tunable blue-green emission. J. Alloy. Compd. vol. 764, 142–146. https://doi.org/10.1016/j.jallcom.2018.06.048.

Schwab, F., Zhai, G., Kern, M., Turner, A., Schnoor, J.L., Wiesner, M.R., 2016. Barriers, pathways and processes for uptake, translocation and accumulation of nanomaterials in plants-Critical review. Nanotoxicology *10* (3), 257–278. https://doi.org/10.3109/17435390.2015.1048326.

Shafqat, U., Hussain, S., Shahzad, T., et al., 2023. Elucidating the phytotoxicity thresholds of various biosynthesised nanoparticles on physical and biochemical attributes of cotton. Chem. Biol. Technol. Agric. 10, 30. https://doi.org/10.1186/s40538-023-00402-x.

Sharma, S.K., Pitale, S.S., Malik, M.M., Qureshi, M.S., Dubey, R.N., 2009. Spectral and kinetic characterisation of orange-red emitting $Sr_3Al_2O_6$:Eu^{3+}/Sm^{3+}phosphor. J. Alloy. Compd. vol. 482 (1–2), 468–475. https://doi.org/10.1016/j.jallcom.2009.04.058.

Su, Yu, Iwasa, Yuki, Yanagida, Takayuki, Tsujimoto, Yoshihiro, Luo, Shunqin, Ogino, Hiraku, 2022. Luminescence properties of Tb-doped $Ba_3Y_2O_5Cl_2$. Opt. Mater. Express 12, 3837–3845.

Thomas, N.M., Sreeja, V.G., Vanchipurackal, I.V., Anila, E.I., 2020. Structural and linear optical properties of blue light emitting Sr3Al2O6. AIP Conf. Proc. vol. 2265 (November), 3–7. https://doi.org/10.1063/5.0016980.

Ullah, H., et al., 2020. In vivo phytotoxicity, uptake, and translocation of PbS nanoparticles in maise (Zea mays L.) plants. Sci. Total Environ. 737, 139558 https://doi.org/10.1016/j.scitotenv.2020.139558.

Vitola, V., Millers, D., Bite, I., Smits, K., Spustaka, A., 2019. Recent progress in understanding the persistent luminescence in $SrAl_2O_4$:Eu,Dy. Mater. Sci. Technol. (U. Kingd.) vol. 35 (14), 1661–1677. https://doi.org/10.1080/02670836.2019.1649802.

Wang, L., et al., 2016. Enhancing photovoltaic performance of dye-sensitised solar cells by rare-earth doped oxide of $SrAl_2O_4$:Eu^{3+}. Mater. Res. Bull. vol. 76, 459–465. https://doi.org/10.1016/j.materresbull.2016.01.013.

Wang, Xueran, et al., 2023. Nanoparticles in plants: uptake, transport and physiological activity in leaf and root. Materials vol. 16 (8), 3097. https://doi.org/10.3390/ma16083097.

Xin, Gui, et al., 2023. Understanding the phytotoxic effects of CeO_2 nanoparticles on the growth and physiology of soybean (Glycine max L. Merrill) in soil media. Environ. Sci.: Nano vol. 10, 2904–2912. https://doi.org/10.1039/D3EN00310H.

Yadav, T., Mungray, A.A., Mungray, A.K., 2014. Fabricated nanoparticles: current status and potential phytotoxic threats. Rev. Environ. Contam. Toxicol. vol. 230, 83–110. https://doi.org/10.1007/978-3-319-04411-8_4.

Yang, Jie, Cao, Weidong, Rui, Yukui, 2017. Interactions between nanoparticles and plants: phytotoxicity and defense mechanisms. J. Plant Interact. 12 (1), 158–169. https://doi.org/10.1080/17429145.2017.1310944.

Zhai, B.G., Huang, Y.M., 2017. Green photoluminescence and afterglow of Tb-doped $SrAl_2O_4$. J. Mater. Sci. 52, 1813–1822. https://doi.org/10.1007/s10853-016-0471-x.

Zhao, L., et al., 2020. Nano-biotechnology in agriculture: use of nanomaterials to promote plant growth and stress tolerance. J. Agric. Food Chem. vol. 68 (7), 1935–1947. https://doi.org/10.1021/acs.jafc.9b06615.

Zheng, L., Hong, F., Lu, S., Liu, C., 2005. Effect of Nano-TiO_2 on strength of naturally aged seeds and growth of spinach. Biol. Trace Elem. Res. vol. 104, 83–91. https://doi.org/10.1385/bter%3A104%3A1%3A083.